*Supporting Information for*

# Moisture transformation in Arctic warm airmass intrusions: process attribution with stable water isotopes

C.F. Brunello [1], F. Gebhardt [1,2], A. Rinke [1], M. Dütsch [3], S. Bucci [3], H. Meyer [1], M. Mellat [1], M. Werner [1]

[1] Alfred Wegener Institute, Helmholtz Centre for Polar and Marine Research, Germany
[2] Institute of Physics and Astronomy, Institute of Environmental Science and Geography, University of Potsdam, Germany
[3] Department of Meteorology and Geophysics, University of Vienna, Vienna, Austria

## Content of this file

Text **S1**
Text **S2**
Figure **S1-S4**

## Introduction

This supporting information provides a more detailed description (Text S1, Figure S1) of the Process Attribution algorithm presented in the main text in Chapter 2.3. Additionally, we provide two supporting figures for the discussion in main text section 4.2. Figure S2 illustrates the correlations of d-excess with contributions of moisture uptake from sea-ice dominated regions and Figure S3 shows the relationship between d-excess and $RH_{sst}$ at the evaporative source regions. Finally, in text S2, we include a complementary analysis where results from the isotope enabled general circulation model ECHAM6-wiso are compared to the isotope observations and the process attributions obtained from ERA5 fields. The results of the analysis are presented in Figure S4, which is directly comparable to Figure 2 in the main text.

## Text S1

### S1.1 Process attribution

In this study, we adapt the moisture attribution algorithm of Duetsch et al., (2018) in order to account for both the attribution of uptakes and losses along the airmass trajectories in the specific dry and cold environmental conditions of the Arctic region. The first step is to identify moisture changes $\Delta q(t)$ at a given timestep along the trajectory. This is done as follows:

$$\Delta q(t) = q(\mathrm{R}x(t)) - q(\mathrm{R}x(t - 3h)) \qquad \text{Eq.1}$$

where $\mathrm{R}x(t)$ is the position of the air parcel at time t (Sodemann et al., 2008).
If $|\Delta q(t)| > \Delta qmin$ the moisture change is attributed to a process. The threshold $\Delta qmin$ is used to reduce noise and was set to 0.01 gkg−1 in Dütsch et al. (2018). We use $\Delta qmin = 0.001$ gkg−1 to account for Arctic dry and cold conditions. The processes are assigned according to the decision tree shown in Figure S1. At humidity change between $t$ and $t$ – 3h, values of each variable, that are used in the decision tree, are averaged over $\mathrm{R}x(t)$ and $\mathrm{R}x(t - 3h)$ to account for small scale temporal and spatial variability.

In case of a positive change in moisture content, the altitude of the air parcel is used to identify if the uptake happened within the BL. To account for local injections of BL moisture through moist convection and for the uncertainty of the BL parametrization of ERA5, the BL height is increased by a factor of 1.5 as in Dütsch et al. (2018). Moisture increases in the free troposphere are considered as the result of vertical or horizontal mixing. Assuming well-mixed conditions in the BL, an uptake located within the BL can be directly attributed to evaporation from the underlying source region. Surface evaporation allows up to four different source areas: land, ocean, and sea ice with and without significant lead fraction. First, evaporation from land masses and evaporation from the ocean are distinguished by using a land-sea mask. Secondly, if the air parcel is located over ocean, the sea-ice concentration is used to detect evaporation over sea ice. This process includes evaporation from open-water bodies within the ice or near sea-ice margins, over polynyas, and sublimation from the snow-covered ice surface. Since evaporation from leads is considered to contribute to enhanced local moistening of the Arctic atmosphere (Wendisch et al., 2023), we further divide our approach into sea ice with lower lead fraction or sea ice with high lead fraction using the lead fraction from the AMSR-2 data set. Due to the small-scale characteristic of leads, the average resulting values vary between 0 and 10 %. The ERA5 data does not resolve leads explicitly in the sea-ice data, so moisture uptakes due to these features are limited. Nevertheless, information about their occurrence along the trajectories can be useful for our isotope analysis.

Moisture losses are due to cloud formation, precipitation by rain or snow and dew formation by vapor deposition. Here, we do not resolve if precipitation occurred and always refer to the different types of cloud formation, knowing that WAIs are often accompanied by significant precipitation (Viceto et al., 2021; Kirbus et al., 2023). A threshold of 80 % RH is used, where sub-grid scale condensation is likely to occur (Dütsch et al., 2018). If RH is below that level, moisture decreases are considered to be the result of vertical and horizontal mixing and are assigned to the process 'mixing out'. If the threshold is exceeded, clouds are likely to form. Based on the temperature of the air parcel, the resulting cloud is liquid (T > 0°C), solid (-23°C > T), or mixed-phase (-23°C<T<0°C).

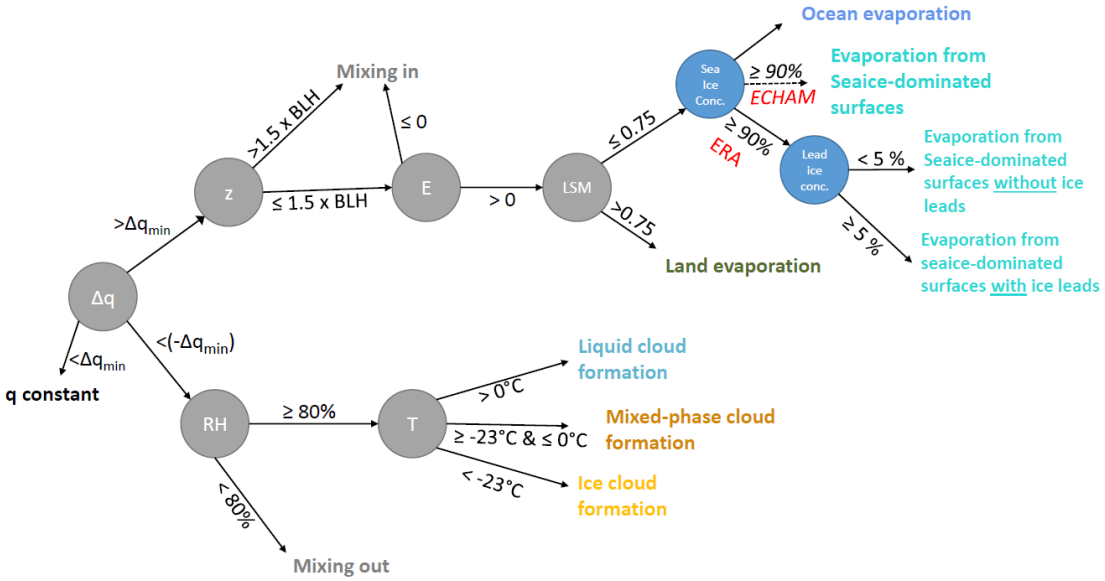


**Figure S1:** *Illustration of the decision tree, which is used to indicate the process types associated with changes of q in the air parcel (modified from Dütsch et al. 2018). The parameters used here are the detected moisture change (> Δqmin), Height (z), Boundary Layer Height (BLH), Evaporation from the surface (E), Land-Sea Mask (LSM), Sea-Ice Concentration (SIC), lead fraction, Relative Humidity (RH) and Temperature (T). If the absolute moisture change is large enough (> Δqmin), the moisture change is allocated to processes associated with uptakes on the upper branch or processes associated with losses on the lower branch. If > Δqmin is not exceeded, q is considered to be constant. The conditions written along the branches indicate the thresholds used to assign a process.*

## S1.2 Moisture weighting

Along its trajectory, an air parcel may experience multiple uptakes and losses. Moisture that originates from an earlier uptake of the air parcel can be fully removed from the air parcel through rain outs and cloud formation and is replaced by later uptakes. Thus, each air parcel arriving at RV Polarstern can be described as a weighted sum of previous uptakes (Sodemann et al., 2008).

A moisture weighting procedure is used to calculate the contribution of each uptake to the moisture content at the target location (Dütsch et al., 2018). At the target location, the amount of moisture is defined as $q^{n=N_{fin}}$, with $N$ being the timestep at target location, and is ideally equal to the observed $q$ at this time. At any timestep $n$, backwards in time along an air parcel's trajectory, the contribution to $q^{N_{fin}}$ is a fraction of its current moisture content defined as $f^{n_{fin}}$. This is calculated using the following equation (Dütsch et al., 2018):

$$f_{fin}^{n} = f_{fin}^{m} \cdot \min\left(\frac{q^m}{q^n}, 1\right), \qquad \text{where m>n} \qquad \text{Eq.1}$$

$$q_{fin}^{n} = f_{fin}^{n} \cdot q^n \qquad \text{Eq.2}$$

Multiplying $f^{n_{fin}}$ with the current amount of moisture $q^n$, gives $q^n{}_{fin}$, which is defined as the amount of moisture at a given timestep $n$ that is preserved in the final amount of moisture at the target location. The calculation works backwards in time, thus n is decreased along the trajectory. At target location with timestep $n = N$, the calculation is initialized with $f^{N}{}_{fin} = f^{m}{}_{fin} = 1$.

In case of an uptake ($q^m/q^n > 1$), the fraction $f^{n}{}_{fin}$ reduces $q^n{}_{fin}$ of the previous timestep. It reflects that the moisture $q^n$ now contributes less to $q^{N}{}_{fin}$, as the uptake of the next timestep $m$ will add additional moisture to the air parcel. In case of a moisture decrease, during precipitation or cloud formation, $f^{n_{fin}}$ is described by:

$$f^{n_{fin}} = f^{m}{}_{fin} \cdot (q^m/q^n) \qquad \text{where } m > n, \text{ and } q^m < q^n \qquad \text{Eq.3}$$

Combining Eq.1 and Eq2, it results that $q^n{}_{fin}$ before a moisture decrease is equal to the one of the next timestep $q^m{}_{fin,}$ and it describes exactly that part of $q^n$ which 'survives' events of precipitation and cloud formation.

The sum of all changes of $q^n{}_{fin}$ is defined as the explained moisture:

$$q_{exp} = \sum_{n=0}^{N-1} \Delta q^{n_{fin}} \qquad \text{Eq.4}$$

where $N$ is the total number of timesteps, (here $N$=40; 5 days x 24h/3h). If the majority of the moisture content at the target location was uptaken later than 5 days before the arrival, $q_{exp}$ is close to $q^N$. In the opposite case, if the majority of the uptakes happened earlier than 5 days before arrival at the target location and only a few uptakes are tracked along the trajectory, $qex\ p$ is low compared to $qN$.

Based on the identified processes and the weights $q^n{}_{fin}$, the weighted sum of all moisture exchanges along the trajectory is calculated based on the weighting presented in Sodemann et al (2008). The changes are integrated along the trajectory ($n \rightarrow N$) for each process ($k$) separately.

$$\Delta q_{total} = \sum_{n=0}^{N-1} \left(\frac{q_{fin}^{n}}{q_{fin}^{N}} \Delta q^{n,k}\right) \qquad \text{Eq.5}$$

Here, $\frac{q_{fin}^{n}}{q_{fin}^{N}}$ is the fraction of moisture at timestep n, which is still contained at the target location and is used as the weighting factor. Finally, the relative contribution of each process to the total amount of moisture exchanges is calculated as follows:

$$\Delta q^{k}{}_{relative} = |\Delta q^{k}{}_{total}| / \sum_{n=0}^{N-1} |\Delta q^{n}| \qquad \text{Eq.6}$$

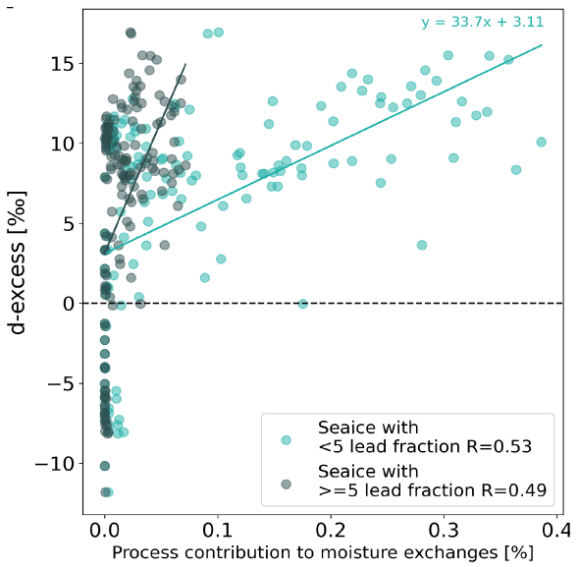


**Figure S2**: *Relationship between the contribution of sea-ice evaporation and d-excess, including both sea ice with high lead fraction and sea ice with lower lead fraction with the respective regression lines. The equation for the regression line of sea ice with low lead fraction is written at the top right.*

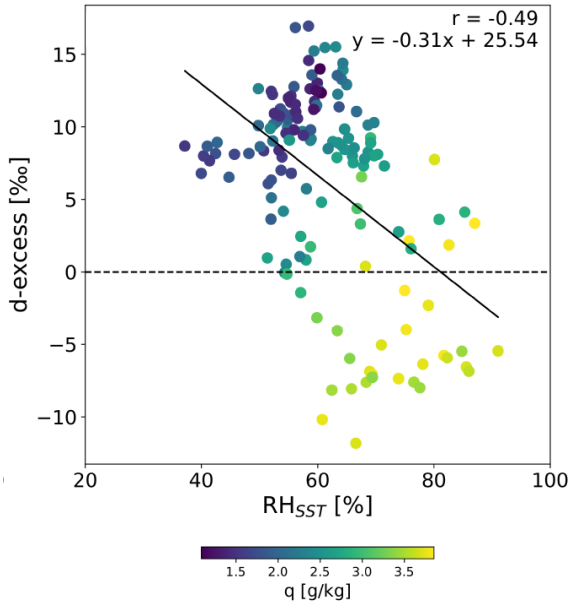


**Figure S3:** *Relationship of d-excess to RH$_{SST}$ for the second peak of the summer case (WAI2a). The color scale indicates the local humidity at RV Polarstern. A linear regression is applied. The relationship has a significant r value (p<0.05) and the equation is given at the top right.*

## Text S2

The process attribution analysis based on ERA5 and presented in the main manuscript was replicated based on meteorological fields from an ECHAM6-wiso simulation with explicit isotope diagnostic (Werner et al., 2011).

Here, we present the results from a single atmosphere model simulation performed at a horizontal grid size of ~0.9 × 0.9 ° and 95 vertical levels (T127L95) (Cauquoin and Werner, 2021). To ensure that the simulated large-scale atmospheric flow is modelled in agreement with the ECMWF reanalysis data, the entire atmospheric column was nudged every 6 h to ERA5 surface pressure, temperature, vorticity and divergence fields. The monthly mean SST and sea-ice fields from the corresponding ERA5 reanalysis have been applied as ocean surface boundary conditions.

### S2.1 Process attribution based on ECHAM6-wiso fields: the winter case

The process attribution, based on ECHAM6-wiso instead of ERA5 fields, yields very similar results for the uptakes (Figure S4a-b). Evaporation from sea ice is slightly larger and contributions from 'mixing-in' are slightly lower compared to ERA5, but the contributions from ocean and land evaporation are nearly identical. However, the processes associated with moisture losses exhibit significant differences. ECHAM6-wiso shows a high contribution of losses caused by 'mixing-out', and a smaller contribution of ice- and mix-phased cloud formation, especially during cold phases. The general shift to mixed-phase cloud formation with the beginning of WAI1 is however captured.

ECHAM6-wiso modelled isotopes (Figure S4d) reveal that the simulated temporal variability of both $\delta^{18}O$ and d-excess is underestimated (std $\delta^{18}O$ = 1.23 ‰, std d-excess = 4.14 ‰) with respect to the observations (std $\delta^{18}O$ = 2.92 ‰, std d-excess = 5.83 ‰). Both variables appear largely overestimated and insensitive to changes in temperature and humidity. Only after the intrusion on Feb 19, simulated $\delta^{18}O$ aligns with the observations. Similarly, during the intrusion, ECHAM6-wiso simulates a d-excess peak along with the peak in temperature, and the stable d-excess signal during the intrusion agrees with the observations.

### S2.2 Process attribution based on ECHAM6-wiso fields: the summer case

Nearly equal process contributions for uptakes are shown by the ECHAM6-wiso simulation as compared to ERA5 (Figure S4e-f). The dominant role of mixed-phase cloud formation in cold phases and the transition to liquid cloud formation during the intrusion are also reproduced. Unlike for ERA5, there is a persistent contribution of 'mixing-out`, accounting for up to 20 % of the moisture exchanges during the WAIs. This additional process contributes on account of the mixed-phase and liquid cloud formation in ERA5. ECHAM6-wiso reproduces day-to-day variations in specific humidity at POL in agreement with the measurements, including the changes associated with the WAIs, but falls short in capturing small-scale variability such as the two humidity peaks on Sep 19 (Figure S4g).

Modelled $\delta^{18}O$ and d-excess values of ECHAM6-wiso (Figure S4h) follow the major evolution of the observations but their simulated variability is underestimated (ECHAM-wiso: std $\delta^{18}O$ = 3.90 ‰, std d-excess = 3.67 ‰; Picarro: std $\delta^{18}O$ = 5.49, d-excess = 6.60 ‰), resulting in large offsets in the absolute values. The $\delta^{18}O$ offset is larger during WAIs (-10 ‰) than during cold-phases (+5 ‰). In contrast to the winter intrusion, large absolute offsets in modelled and measured d-excess are found in the two simulated WAI2 (+10-15 ‰), and better results are obtained during cold phases, although variability is not accurately simulated. The anticorrelation between $\delta^{18}O$ and d-excess is generally captured (r = -0.92), but this relationship is weaker during the first WAI, where modelled d-excess values remain stable around +10 ‰.

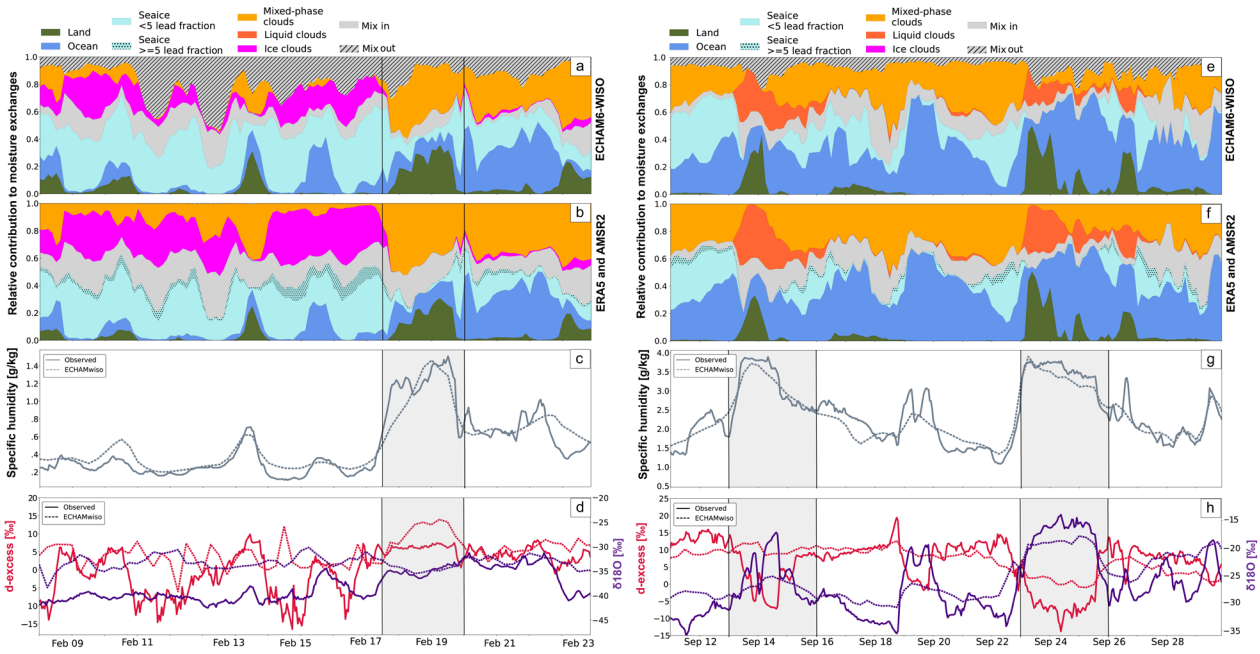


**Figure S4:** *Results of the process attribution diagnostic for the winter case (left) and summer case (right) based on ECHAM6-wiso (a-e), and compared to the results obtained from ERA5 fields (b-f). WAI1, WAI2a and WAI2b are highlighted by vertical black lines. In the middle panels (c-g), modelled and observed local humidity at POL are shown. The lowest panels (d-h) present observed local d-excess and $\delta^{18}O$ as measured by the CRDS onboard POL and the near-surface corresponding variables as modelled by ECHAM6-wiso.*

## S2.3 Considerations on model biases

The process attribution only considers humidity, RH and temperature to determine cloud formation and cloud type, which limits a detailed interpretation. Nonetheless, it is interesting to note that ECHAM6-wiso correctly simulates the total vapor mixing ratios (Figure S4c-g), but the lack of moisture loss due to cloud formation is balanced by the process 'mixing out'. Moisture removals are attributed to 'mixing out' rather than could formation if RH is underestimated by ECHAM6-wiso. This is in contradiction with Kretzschmar et al., (2019) who found that ECHAM6 generally overestimates RH in the Arctic and has a positive bias in liquid cloud formation. However, comparing modelled and observed RH, we found an underestimation of RH in ECHAM6-wiso, along the 80% RH threshold. ECHAM6-wiso calculates grid cloud fraction based on grid mean RH, giving the basis for the calculation of cloud ice and liquid water content (Giorgetta, 2013). Isotope fractionation in clouds are then modelled as equilibrium fractionation which depends on the ice and liquid phase within the cloud. Hence, wrong estimates of cloud water contents could account for underestimations of $\delta^{18}O$ values. For the representation of d-excess in the Arctic, the parametrization of ice growth under super saturation is key. ECHAM6-wiso does not allow the explicit simulation of supersaturation over ice and parameterizes the Bergeron-Findeisen process via a threshold in cloud ice water (Giorgetta, 2013). Kretzschmar et al., (2019) improved the cloud representation significantly by adding such supersaturation process with respect to ice. However, this improvement is not included in the default model release of ECHAM6-wiso used in this study. In conclusions, all these biases, including an over-estimation of liquid water content in ECHAM6-wiso, underestimations of RH linked to cloud water contents, and positive temperature biases in ERA5 fields used for the nudged ECHAM6-wiso simulation used in this study, are likely to cause the ECHAM6-wiso model offsets in d-excess and in $\delta^{18}O$.